JOURNAL OF MATERIALS SCIENCE **36** (2001) 2089–2094

The effect of Fe on the crystallization behavior of Al–Mm–Ni–Fe amorphous alloys

H. W. JIN, Y. J. KIM, C. G. PARK
Center for Advanced Aerospace Materials, Pohang University of Science & Technology, 790-784, Pohang, Korea
E-mail: cgpark@pastech.ac.kr

The crystallization behavior and thermal stability of $Al_{86}Mm_4Ni_{10-x}Fe_x$ alloys were investigated as a function of Fe content. Alloys, produced by a single roll melt-spinner at a circumferential speed of 52 m/s, revealed fully amorphous structures. The thermal stability of the present amorphous alloys increased with the increase of Fe content. The activation energy for crystallization of α-Al increased as the Fe content increased. This increase of activation energy resulted in the simultaneous precipitation of α-Al and intermetallic phase observed especially in $Al_{86}Mm_4Ni_5Fe_5$ and $Al_{86}Mm_4Ni_2Fe_8$ alloys. The glass transition was observed in DSC thermogram only after proper annealing treatment. The effect of alloy composition on the thermal stability could be explained in terms of the atomic structure of the amorphous alloy.

1. Introduction

Amorphous aluminum alloys have been attractive because of their high tensile strength and low density. Amorphous ternary alloys of Al–RE–TM (RE : rare earth element and TM : transition metal) show the tensile strength up to 1560 MPa, which is approximately 3 times higher than that of the commercial crystalline Al-based alloys [1–4]. However, the aluminum-based alloys require high cooling rates in order to make a given alloy in amorphous state. Applications of these amorphous alloys are limited to relatively low temperature (below 200 °C) because they become brittle upon crystallization when exposed at high temperature. However, the crystallization behavior of the present amorphous alloy system is not completely understood yet. Recently, it was reported that the thermal stability of Al–RE–Ni ternary amorphous alloys was substantially improved by partial substitution of Ni with other transition metals, such as Fe, Mn and Co [4, 5], although the mechanism of the enhancement in thermal stability of amorphous phase is not clear. In this article, we report the effect of Fe addition on the thermal stability of amorphous Al–Mm–(Ni, Fe) alloys with systematic change in the relative composition of TM elements. Misch-metal (Mm) was chosen because it is much less expensive than pure RE elements.

2. Experimental procedures

$Al_{86}Mm_4Ni_{10-x}Fe_x$ ($x = 0$, 2, 3, 5, 8, 10 at.%) alloy ingots were prepared by arc melting under argon atmosphere. Starting materials were highly pure elemental granules (99.99% Al, Ni, Fe) and Ce-rich misch-metal (Mm). Alloy ingots were remelted several times in order to homogenize alloy compositions. Then, these alloy ingots were melt-quenched into an amorphous state by using a single-roll melt-spinner in vacuum. The copper roll was 250 mm in diameter and the rotation speed was 4000 rpm. Amorphous alloy ribbons with 2 mm in width and 30 μm in thickness were fabricated.

Amorphous structure of rapidly solidified ribbons was examined by Rigaku X-ray diffractometer. Thermal analysis was carried out in the differential scanning calorimetry (Perkin-Elmer DSC-7) at various heating rates under flow of N_2 gas. DSC samples were prepared in Al capsules. Some alloy specimens are isothermally annealed for 20 minutes at several different annealing temperature below T_{x1}. Isothermal annealing treatment was carried out in DSC and each sample was cooled to 50°C at a cooling rate of 200 K/min. After isothermal heating treatment the sample was reheated at 20 K/min or 40 K/min of scanning rate.

TEM observation was performed on a JEOL 200CX TEM equipped with an in-situ heating holder. Thin foil samples were obtained by twin-jet polishing in a solution of 25% nitric acid and 75% methanol at 243 K. X-ray photoemission spectroscopy (XPS) spectra were also obtained from some alloy ribbons with a Perkin-Elmer PHI 5400 system using Mg K_α radiation.

3. Results and discussion

Fig. 1 shows X-ray diffraction patterns of the melt-spun $Al_{86}Mm_4Ni_{10-x}Fe_x$ ($x = 0$, 2, 3, 5, 8, 10) amorphous ribbons. Only broad diffusive peaks are observed in each specimen as shown in Fig. 1. These broad peaks indicate that fully amorphous structure could be obtained in the rapidly solidified alloy ribbons.

Fig. 2 exhibits the DSC thermogrms of the present amorphous alloy ribbons. The first crystallization temperature (T_{x1}) increased with the increase of Fe content. And significant differences were observed depending

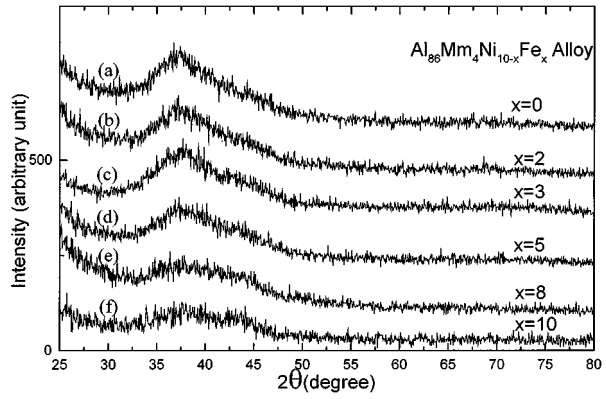

Figure 1 X-ray diffraction patterns of the rapidly solidified $Al_{86}Mm_4Ni_{10-x}Fe_x$ alloys with varied x values: (a) $x = 0$, (b) $x = 2$, (c) $x = 3$, (d) $x = 5$, (e) $x = 8$ and (f) $x = 10$.

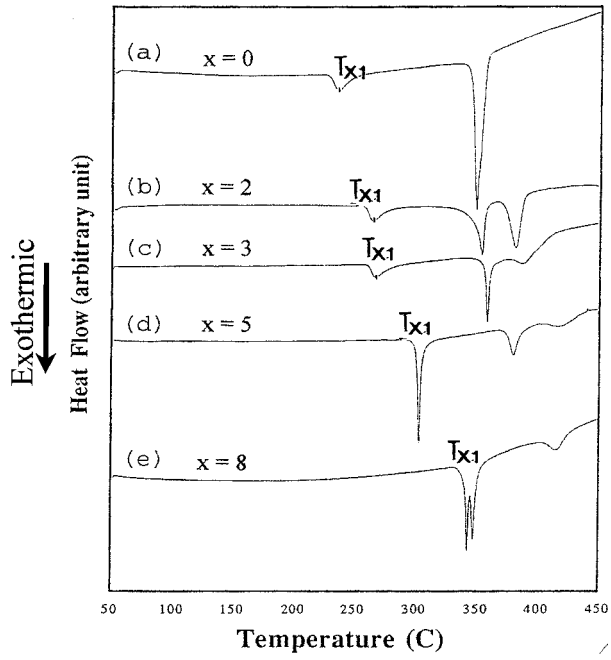

Figure 2 DSC thermograms for $Al_{86}Mm_4Ni_{10-x}Fe_x$ amorphous alloys at a constant heating rate of 20 K/min; (a) $x = 0$, (b) $x = 2$, (c) $x = 3$, (d) $x = 5$ and (e) $x = 8$.

on the Fe content in DSC heating curves shown in Fig. 2. In the alloys containing less than 3 at.% Fe, a small exothermic peak was followed by a sharp exothermic peak. The second sharp exothermic peak appeared at a temperature about 100 K higher than that of the first one. X-ray diffraction results revealed that the first small exothermic peak corresponded to the crystallization of α-Al from amorphous phase and the following exothermic peaks corresponded to the crystallization of some intermetallic phases such as Al_3(Ni, Fe) and $Al_{11}Ce_3$ [6]. On the other hand, alloys containing 5 at.% Fe and 8 at.% Fe exhibited narrow first exothermic peaks.

The lowest crystallization temperature, T_{x1}, defined as the onset temperature of the first exothermic peaks in Fig. 2a–d, shows a nearly linear relationship with the Fe content. Fig. 3 shows the Kissinger plot of the first exothermic peaks in the DSC results. The activation energy of the α-Al precipitation, evaluated from the slope of linearity in Kissinger plot, is 2.47 eV

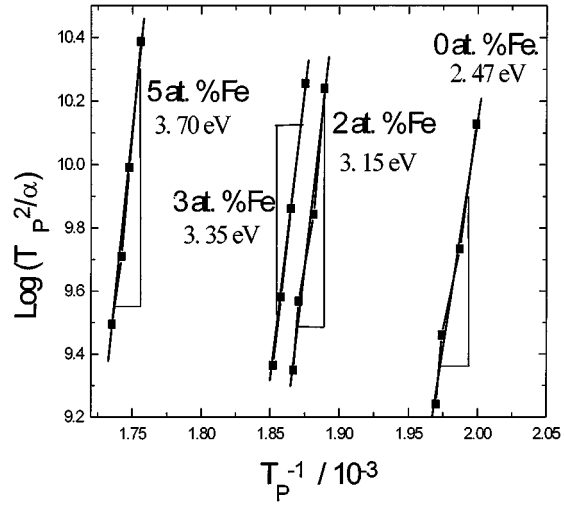

Figure 3 Kissinger plots for the first exothermic peaks in DSC thermograms of the present alloy ribbons.

for the $Al_{86}Mm_4Ni_{10}$ alloy and increases substantially with increasing Fe content, x. The activation energy of the first crystallization reaches a value of 3.70 eV in $Al_{86}Mm_4Ni_5Fe_5$ alloy. In some of the Al-based amorphous alloys, the growth of α-Al without nucleation was proposed as a first crystallization reaction due to the presence of quenched-in nuclei [7]. In the present study, however, the activation energy of crystallization is much higher than that of Al self-diffusion ($\sim$1.45 eV). Thus, the nucleation and growth mechanism can explain the crystallization of α-Al in the present study.

It was reported that there is a strong interaction between Al atom and Fe atom in amorphous Al–RE–Fe alloys [8, 9]. From the small angle X-ray and neutron scattering results, it was suggested that Fe atoms are surrounded by many Al atoms within 3 Å range in close contact with Fe atoms in Al–Ce–Fe system. While rare earth atoms are basically randomly distributed except that they are repelling each other. Therefore, the activation energy for the precipitation of α-Al also increased with an increase of Fe content because Al atoms should overcome the binding energy of strong Al–Fe bonds to form nuclei of α-Al.

Fig. 4 shows the microstructure of the alloy ribbons after the first crystallization peak. Only α-Al was observed in the alloys of $x = 0$, 2 and 3. The presence of some dendrite particles in $Al_{86}Mm_4Ni_7Fe_3$ alloys indicates the relatively low nucleation frequency of α-Al than in the $Al_{86}Mm_4Ni_5Fe$ alloy ribbons. However, some intermetallic phases such as Al_3(Ni, Fe), indicated by arrows in electron diffraction pattern of Fig. 4b, were observed in the alloys of $x = 5$.

TEM studies with *in situ* isothermal heating were conducted at the temperature of the first crystallization peak in DSC heating curves. The *in situ* isothermal annealing results, shown in Fig. 5, exhibits the crystallization process of $Al_{86}Mm_4Ni_5Fe_5$ amorphous alloy ribbons. It was found that the α-Al and intermetallic phases precipitated simultaneously. Thus the first exothermic peak observed in $Al_{86}Mm_4Ni_5Fe_5$ alloy can be regarded as overlapping of the peaks for the precipitation of α-Al and intermetallic phases.

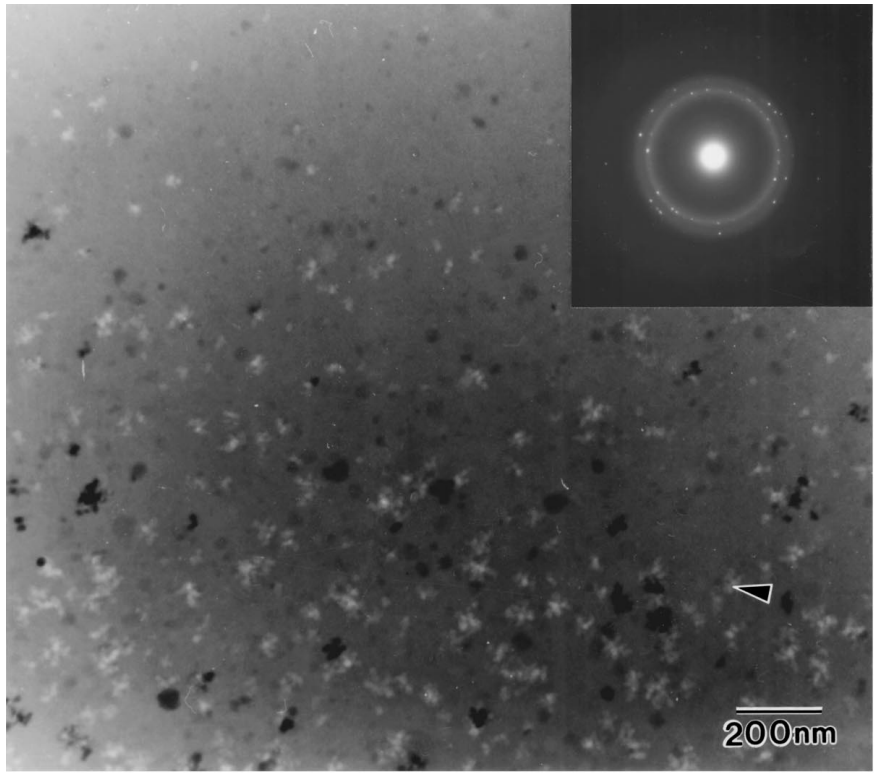

(a)

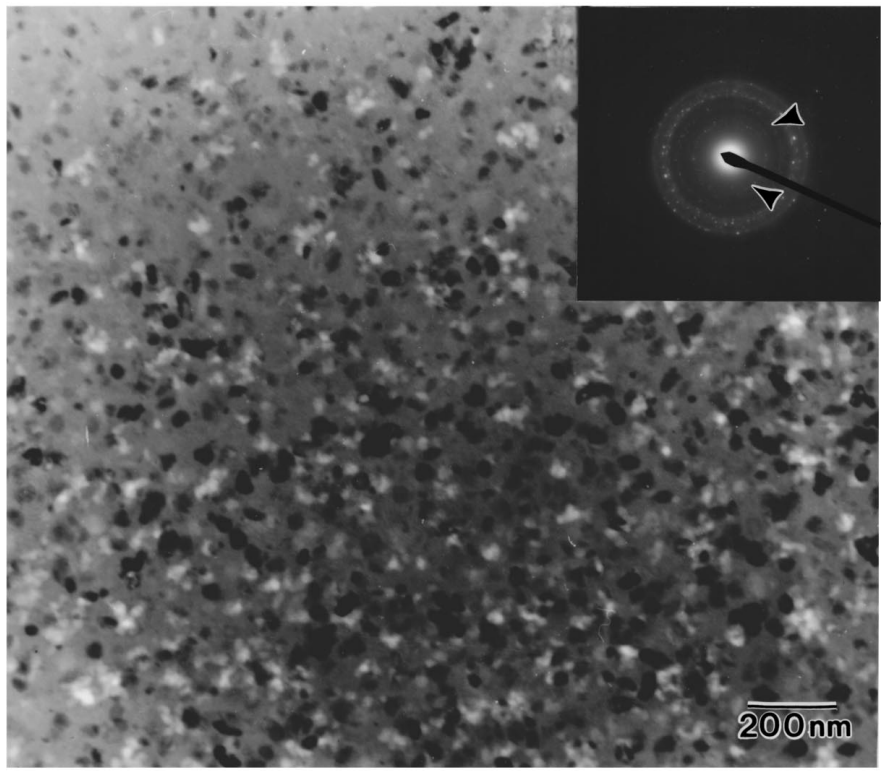

(b)

Figure 4 Bright-field TEM micrographs and electron diffraction patterns showing the crystallization products after first exothermic peak in DSC curves of $Al_{86}Mm_4Ni_7Fe_3$ (a) and $Al_{86}Mm_4Ni_5Fe_5$ (b).

It is noted that the specimen does not show any endothermic step, i.e. glass transition (T_g), before crystallization. The glass transition has been most widely used calorimetric evidence of amorphous materials. However, the absence of glass transition in DSC scans does not necessarily imply that the material is not really amorphous or is microsystalline. For some amorphous alloys, glass transition was not observed though it was absolutely fully amorphous [10–12]. A. Inoue *et al*. [10] suggested that the absence of glass transition temperature (T_g) implies that glass transition temperature is higher than the crystallization temperature (T_x). The glass transition during differential scanning calorimetry can be described as a kinetic phenomenon caused by

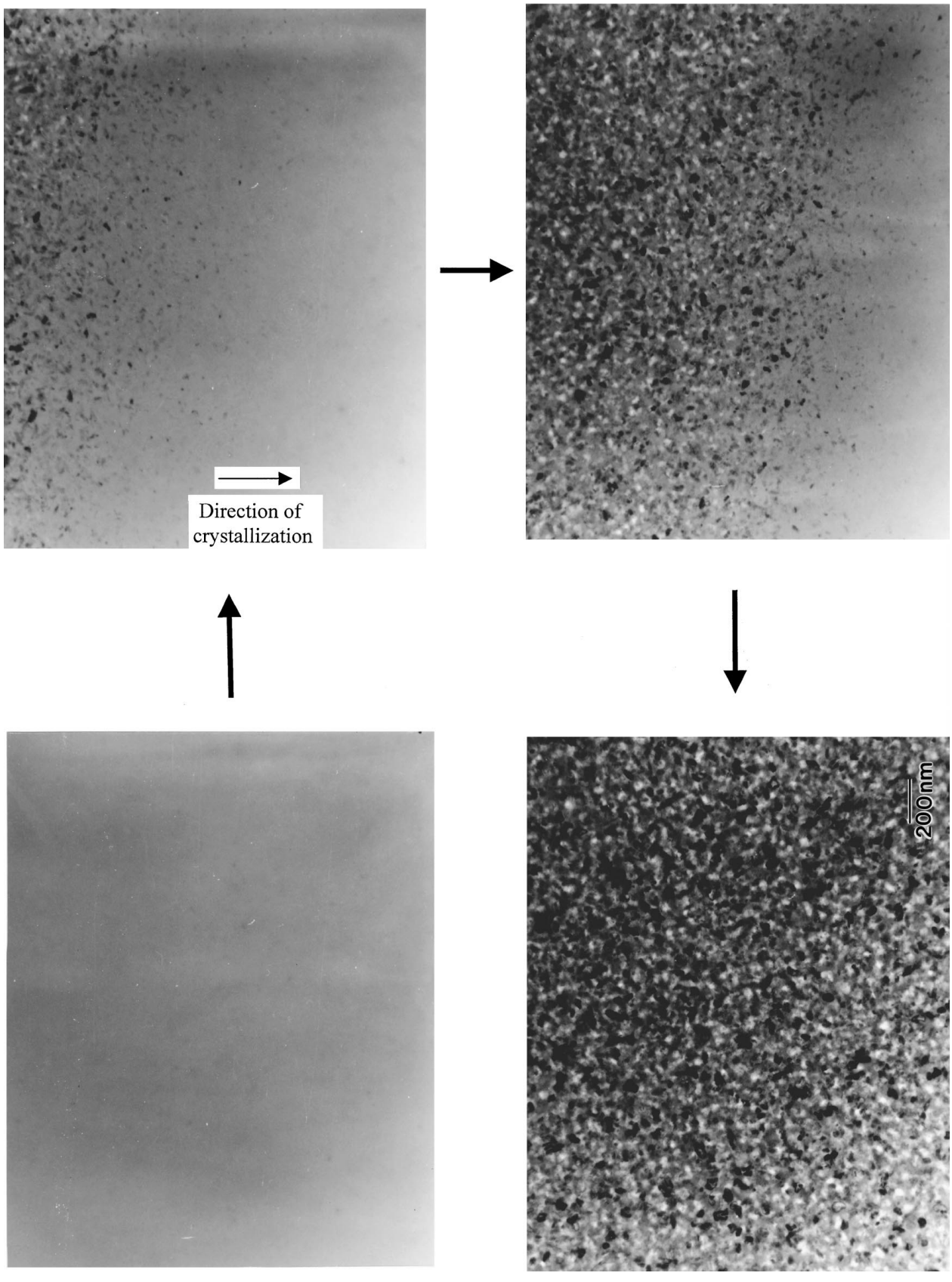

Figure 5 Bright-field TEM micrographs and electron diffraction patterns showing the propagation of crystallization front in the in-situ heating experiment of first crystallization peak of amorphous $Al_{86}Mm_4Ni_5Fe_5$ alloy.

the continuous approach of free volume towards equilibrium during the warming up. Thus, it seems out of reason to consider that crystallization can take place, which requires long-range diffusion of constitute atoms and the formation of critical size of nuclei, while maintaining excess free volume far from equilibrium state. Some researchers, such as R. F. Cochrane [11] and A. Inoue [12], supposed that T_g might not be observed if crystallization occurred only by growth mechanism from the quenched-in α-Al nuclei. In the present study,

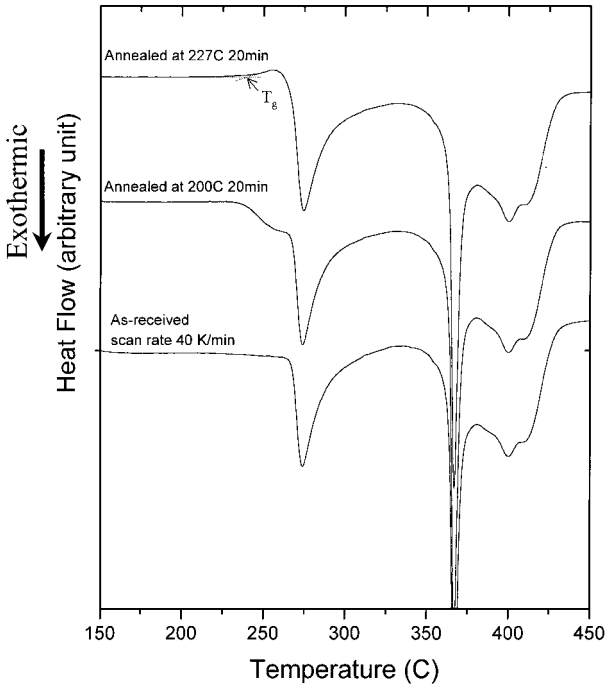

Figure 6 DSC thermograms recorded after isothermal annealing at different annealing temperatures of $Al_{86}Mm_4Ni_7Fe_3$ amorphous alloy.

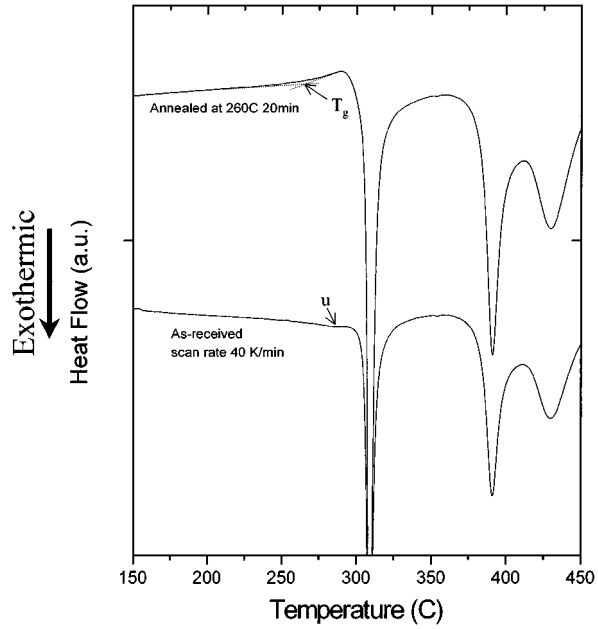

Figure 7 DSC thermograms recorded after isothermal annealing at 260 °C for 20 min with scanning rate of 40 K/min.

however, no quenched-in nuclei could be found in TEM observations in the as-quenched alloy ribbons. And the activation energy for the first crystallization, evaluated in the present investigation, is much greater than that of Al self-diffusion. Thus, a new viewpoint is necessary in order to explain the crystallization behavior of the present alloy system. The present authors suggest that glass transition may be obscured by other exothermic reactions since the glass transition of a particular material partly depends on its thermal history. That is, small exothermic peak due to the glass transition may be obscured when other heat evolving reactions—such as structural relaxation—occur near the glass transition. Fortunately, these heat evolution reactions can be removed by proper pre-annealing heat treatment.

Fig. 6 shows the DSC scans of the alloy containing 3 at.% Fe before and after annealing treatment. The DSC scan of as-quenched specimen exhibits almost steady heat flow, i.e. nearly flat baseline, before crystallization. However, DSC scans of isothermally annealed specimen exhibited an endothermic step, i.e. the glass transition. These results imply that the glass transition occurs on heating the present alloy ribbons although it was not detected in conventional DSC scans and the exothermic step of glass transition was masked by some exothermic reactions near the crystallization temperature range. The observation of endothermic step (T_g) was more pronounced at higher annealing temperature because the exothermic reaction can be effectively eliminated by annealing at higher temperature.

In the crystallization by nucleation and growth mechanism, pre-annealing heat treatment may result in partial crystallization [13]. Thus, a peak shift to low temperature would be observed in sub-sequent DSC scanning. In case of crystallization by growth mechanism, on the other hand, peak shift toward high temperature would be observed because pre-annealing increase the grain size of quenched-in nuclei [13]. In the present investigation, no peak shift could be recognized in subsequent DSC scanning after pre-annealing heat treatment. This result, thus, may exclude the possibility of partial crystallization of amorphous phase or grain growth of quenched-in nuclei during the pre-annealing heat treatment.

The glass transition was also observed in the alloys containing 5 at.% Fe after pre-annealing heat treatment as shown in Fig. 7. Increase in scanning rate revealed a broad exotherm, designated as 'u', in the DSC thermogram from as-quenched specimen. And this broad exotherm disappeared after isothermal pre-annealing heat treatment. This result is a strong evidence for the masking of glass transition by exothermic structural relaxation.

Fig. 8 shows the XPS spectra from some alloy ribbons near the Al 2p level (72.9 eV). Only one sharp peak, designated as "α", appears in as-quenched ribbons. The binding energy of "α" peak corresponds to 72.8 eV,

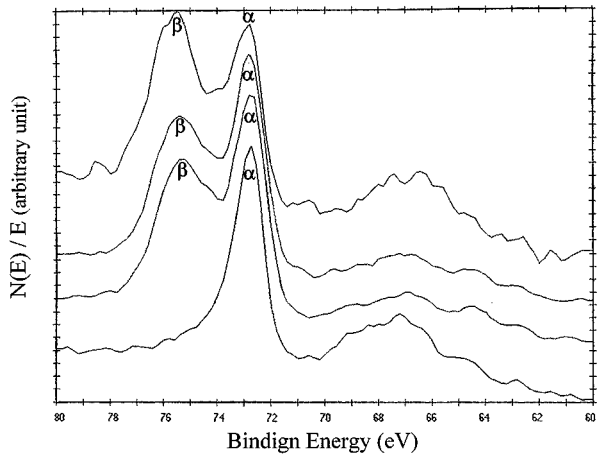

Figure 8 XPS spectra of the $Al_{86}Mm_4Ni_7Fe_3$ alloy ribbons with different heat treatment conditions. (a) as-quenched, (b) annealed at 200 °C for 20 min., (c) annealed at 227 °C for 20 min. (d) annealed to 450 °C.

which is quite close to that of pure Al (72.9 eV). In pre-annealed specimen, a new peak—denoted as "β"—is observed in addition to original "α" peak. The binding energy of "β" peak is about 75.4 eV, 2.6 eV higher than that of "α" peak. And the "β" peak exhibited higher intensity than "α" peak in fully crystallized alloy ribbons after DSC scanning to 450°C. These results indicate that pre-annealing heat treatment caused the structural relaxation of amorphous phase to evolve two different chemical environments of Al, i.e. Al-rich region and Al-poor region. And the evolution of structurtuctural relaxation is followed by the precipitation of α-Al and intermetallic phase such as (Ni, Fe)Al_3, and $Al_{11}Mm_3$ in the two chemically different regions respectively. The substitution of Ni with Fe enhances this kind of structural relaxation since Fe has stronger interaction with Al than Ni has.

4. Conclusion

1. The thermal stability of the present amorphous alloys was enhanced by the addition of Fe.

2. Primary crystallization of α-Al was the first crystallization product in the alloys containing small fraction of Fe upto 3 at.%. Further increase of Fe content above 5 at.% induced eutectic crystallization of α-Al and some intermetallic phase as a first crystallization reaction.

3. The glass transition was obscured by exothermic heat evolution caused by structural relaxation. By implying suitable heat treatment, the glass transition could be observed in DSC thermograms.

References

1. A. INOUE, Y. H. KIM and T. MASUMOTO, *Mater. Trans. JIM* **33** (1992) 487.
2. A. INOUE, Y. HORIO, Y. H. KIM and T. MASUMOTO, *Mater. Trans. JIM* **33** (1992) 669.
3. Y. HE, G. M. DOUGHERTY, G. J. SHIFLET and S. J. POON, *Acta Metall. Mater*. **41** (1993) 337.
4. Y. H. KIM, A. INOUE and T. MASUMOTO, *Mater. Trans. JIM* **32** (1991) 559.
5. M. YEWONDWOSSEN, R. A. DUNLAP and D. J. LLOYD, *J. Phys. Condens. Matter*. **4** (1992) 461.
6. H. W. JIN, Y. J. KIM, C. G. PARK and M. C. KIM, in "Light Weight Alloys for Aerospace Applications IV," edited by E. W. Lee, W. E. Frazier, N. J. Kim and J. Nata (1996) 31.
7. A. P. TSAI, T. KAMIYAMA, Y. KAWAMURA, A. INOUE and T. MASUMOTO, *Acta Mater*. **45** (1997) 1477.
8. H. Y. HSIEH, B. H. TOBY, T. EGAMI, Y. HE, S. J. POON and G. J. SHIFLET, *J. Mater. Res*. **5** (1990) 2307.
9. H. Y. HSIEH, T. EGAMI, S. J. POON and G. J. SHIFLET, *J. Non-Cryst. Solids* **135** (1991) 248.
10. A. INOUE, T. ZHANG, W. ZHANG and A. TAKEUCHI, *Materials Transactions JIM* **37** (1996) 108.
11. R. F. COCHRANE, P. SCHUMACHER, A. L. GREER, *Mat. Sci. & Eng. A* **133** (1991) 367.
12. K. NAKAZATO, Y. KAWAMURA, A. P. TSAI and A. INOUE, *Appl. Phys. Lett*. **63** (1993) 2644.
13. L. C. CHEN and F. SPAEPEN, *Mat. Sci. & Eng. A* **133** (1991) 367.

Received 12 February 1999
and accepted 30 August 2000